 CMES, vol.66, no.1, pp.53-71, 2010

An Analysis of Backward Heat Conduction Problems Using the Time Evolution Method of Fundamental Solutions

C.H. Tsai[1], **D.L. Young**[2] **and J. Kolibal**[3]

Abstract: The time evolution method of fundamental solutions (MFS) is proposed to solve backward heat conduction problems (BHCPs). The time evolution MFS belongs to one of the mesh-free numerical methods and is essentially composed of a sequence of diffusion fundamental solutions which exactly satisfy the heat conduction equations. Through correct treatment of temporal evolution, the resulting system of the time evolution MFS is smaller, and effectively decreases the possibility of ill-conditioning induced by such strongly ill-posed problems. Both one-dimensional and two-dimensional BHCPs are examined in this study, and the numerical results demonstrate the accuracy and stability of the MFS, especially for the BHCPs with high levels of noise. Conclusively, time evolution MFS is a stable and powerful numerical scheme, and is especially suitable for the numerical solution of BHCPs.

Keywords: Method of fundamental solutions, backward heat conduction problem, ill-posed problem, diffusion fundamental solutions.

1 Introduction

Meshless numerical methods have been developed as alternatives to the classical mesh-dependent numerical methods, such as the finite-element method (FEM) and finite-difference method (FDM). The method of fundamental solutions (MFS) was initially proposed by Kupradze and Aleksidze (1964). Due to the high efficiency and high accuracy of this method, many researchers adopted MFS to solve various

[1] Department of Civil Engineering & Hydrotech Research Institute National Taiwan University, Taipei, 10617, Taiwan.

[2] Corresponding author. E-mail: dlyoung@ntu.edu.tw. Tel & Fax: +886-2-23626114, Department of Civil Engineering & Hydrotech Research Institute National Taiwan University, Taipei, 10617, Taiwan.

[3] E-mail: joseph.kolibal@usm.edu, Department of Mathematics, The University of Southern Mississippi, Hattiesburg, MS 39406-0001, USA.

engineering problems, including potential [Fenner (1991)], acoustic [Koopmann, Song, and Fahnline (1989)], elastostatics problems [Karageorghis and Fairweather (2000)], biharmonic problem [Smyrlis and Karageorghis (2003)], scattering problems of electromagnetic waves [Young and Ruan (2005)] and inverse problem [Hon and Wei (2005); Marin (2008a,b)].

In general, the MFS method is a boundary-type method, and is composed of the fundamental solutions which exactly satisfy the governing equations. Therefore, it is only necessary to approximate the augmented boundary when MFS is used to solve problems. On the other hand, the MFS can also be regarded as an indirect Trefftz method [Trefftz (1926); Kita and Kamiya (1995)], moreover, compared with boundary element method (BEM), this numerical method is free from singularities and the need for numerical integration. The accuracy of MFS, however, is affected by the ill-conditioning of resulting linear equations system. Liu (2008) proposed a modified MFS to improve the ill-conditioning of the MFS for two-dimensional Laplace equation. In terms of unsteady problems, Young, Tsai, and Fan (2004); Young, Tsai, Murugesan, Fan, and Chen (2004) further solved the multi-dimensional diffusion equations with diffusion fundamental solutions. Besides, Hu, Young, and Fan (2008) extended MFS to solve diffusion equation with unsteady forcing function. By directly using the diffusion fundamental solutions via time evolution, the diffusion equations can be obtained without adopting special techniques to deal with the time-derivative term. Since the solutions within every time evolution process exactly satisfy the governing equations, the solutions in each time step can be obtained accurately. Therefore, reasonable results can be obtained by fewer computational points. In other words, problems are able to be solved by a small resulting linear system instead of a large one which is known to easily cause the problems to be ill-conditioned.

Generally speaking, BHCPs are so ill-conditioned that solutions cannot be obtained directly by classical numerical method without special techniques. The investigation of BHCPs includes the BEM [Han, Ingham, and Yuan (1995)], the iterative BEM [Mera, Elliott, Ingham, and Lesnic (2000), Lesnic, Elliott, and Ingham (1998)], regularization techniques [Muniz, de Campos Velho, and Ramos (1999); Muniz, Ramos, and de Campos Velho (2000)], the group preserving scheme (GPS) [Liu (2004)], the backward group preserving scheme (BGPS) [Liu, Chang, and Chang (2006), Chang and Liu (2010)], the new Lie group shooting method (LGSM) [Chang, Liu, and Chang (2007)], and the MFS [Mera (2005); Hon and Li (2009)]. Indeed, any method that can successfully solve these types of problems merits further consideration and study.

Mera (2005) first used MFS approach to solve BHCPs. Some acceptable solutions are obtained by combining the MFS with standard Tikhonov regularization.

Hon and Li (2009) developed a new method based on the discrepancy principle for choosing the optimal location of source points. This improvement greatly promotes the accuracy and the stability for Mera (2005). Comparing the time evolution MFS proposed by Young, Tsai, and Fan (2004); Young, Tsai, Murugesan, Fan, and Chen (2004) with the approaches presented by Mera (2005) and Hon and Li (2009) , the time evolution scheme considers the diffusion fundamental solutions within each time step instead of the entire space-time domain. Therefore, using fewer collocation points is able to attain accurate results. Moreover, the condition number of the resulting linear system is smaller, and can effectively decrease the ill-conditioning caused by BHCPs. In this investigation, the time evolution MFS presented by Young, Tsai, and Fan (2004); Young, Tsai, Murugesan, Fan, and Chen (2004) is chosen to solve BHCPs. Accurate and stable results are obtained to demonstrate the time evolution MFS is more appropriate to be applied on the BHCPs.

Throughout this study, we adopt the time evolution MFS to apply on BHCPs in 1D and 2D geometries. The governing equations are listed and explained in Section 2. In Section 3, the numerical discretization of the MFS with time evolution scheme is discussed. Moreover, the comparisons of the present results with the analytical solutions and other numerical results are presented in Section 4, and these demonstrate considerable improvement over current methods in solving these types of problems. The conclusions are presented in Section 5.

2 Mathematical formulation

We consider the following equations:

$$\text{PDE:} \quad u_t(\vec{x},t) = \nu\nabla^2 u(\vec{x},t), \qquad \vec{x}\in\Omega, T \geq t \geq 0, \tag{1}$$

$$\text{BC:} \quad u(\vec{x},t) = f(t), \qquad \text{for } \vec{x}\in\partial\Omega, T \geq t \geq 0, \tag{2}$$

$$\text{FC:} \quad u(\vec{x},T) = g(\vec{x}), \qquad \text{for } \vec{x}\in\Omega, \tag{3}$$

where $\Omega \subset \mathbb{R}^d$, $d = 1,2,\ldots,n$, and n is the number of the spatial dimension. In (1)–(3), t is the time variable, $u(\vec{x},t)$ is the heat distribution, ν is the diffusion coefficient, and $f(t)$ and $g(\vec{x})$ prescribe the heat distribution on the boundary and the heat distribution at time T, respectively. The task is to recover the initial heat contribution, $u(\vec{x},0)$, by using the known heat distribution $g(\vec{x})$ at time T.

3 Method of fundamental solutions (MFS)

The solutions of MFS for diffusion equation can be represented as a linear combination of the fundamental solutions given by Kythe (1996),

$$\frac{\partial G(\vec{x},t;\vec{\xi},\tau)}{\partial t} = \nu\nabla^2 G(\vec{x},t;\vec{\xi},\tau) + \delta(\vec{x}-\vec{\xi})\delta(t-\tau), \tag{4}$$

where G is the Green's function, τ is the specific time of the source points, $\vec{x} \in \mathbb{R}^d$ are the locations of the field points, and $\vec{\xi}$ are source points corresponding to t and τ, respectively.

Using Fourier transforms with respect to $\vec{x}$ and Laplace transforms in t, and inverting the transform of (4), the fundamental solution of the diffusion equation can be obtained as the free space Green's function,

$$G(\vec{x},t;\vec{\xi},\tau) = \frac{e^{-(\vec{x}-\vec{\xi})^2/4\nu(t-\tau)}}{[4\pi\nu(t-\tau)]^{d/2}} H(t-\tau), \tag{5}$$

where H is the Heaviside step function. Because the fundamental solutions must satisfy the homogeneous heat conduction equation, the solutions can be written as a linear combination of the fundamental solutions of the heat conduction operator. Thus, the numerical solution of the heat conduction equation can be presented as [Young, Tsai, and Fan (2004); Young, Tsai, Murugesan, Fan, and Chen (2004)]

$$U(\vec{x},t) = \sum_{j=1}^{N_i+N_b} \alpha_j G(\vec{x},t;\vec{\xi}_j,\tau_j), \tag{6}$$

where $U(\vec{x},t)$ is the heat distribution obtained by MFS, and N_i and N_b are the number of the source points specified as initial and boundary points, respectively, and α are undetermined coefficients which can be obtained using the method of collocation so as to satisfy the initial and boundary conditions.

Based on the successful implementation of the forward problems by Young, Tsai, and Fan (2004); Young, Tsai, Murugesan, Fan, and Chen (2004), we considered this time evolution MFS to solve the BHCPs. Because the MFS is used to solve a backward problem, (6) needs to be changed into the following form

$$U(\vec{x},t) = \sum_{j=1}^{N_f+N_b} \alpha_j G(\vec{x},t;\vec{\xi}_j,\tau_j), \tag{7}$$

where N_f and N_b are the number of the source points specified as field points at the given time $t = T$ and boundary points, respectively, and α are undetermined

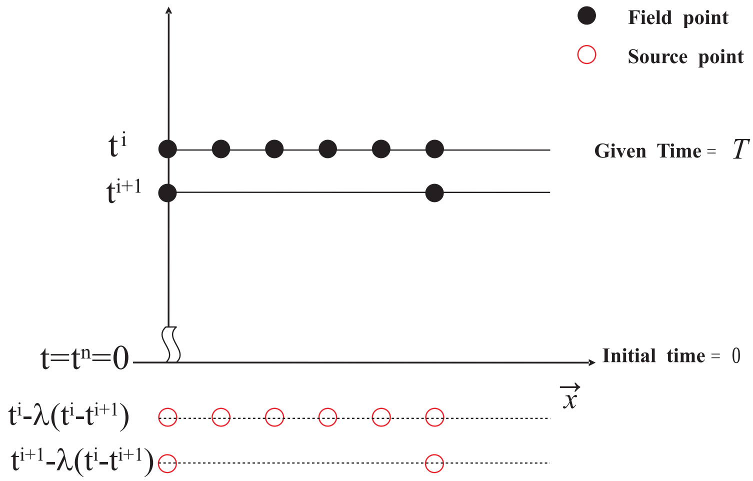

Figure 1: Schematic diagram for the locations of field points and source points on the space-time domain.

coefficients which also can be determined by the method of collocation satisfying the field values at the given time and boundary conditions. Obviously, the process, compared to the forward problem, is to use the given conditions at time $t = T$ instead of at the initial time. Fig. 1 shows the distributions of the field points and the source points in detail in the case of space dimension, $\vec{x}$. In terms of the positions of the field points, the boundary parts of field points are located at the temporal level of $t = t^{i+1}$, and the interior domain of field points are located at the temporal level of $t = t^i$, where $i = 1, n-1$ and $t = t^n = 0$ is the initial time. The source points and the field points are placed at the same positions in space but different in time.

For example, as illustrated in Fig. 1, the boundary parts of source points are located at the temporal level of $t = t^{i+1} - \lambda(t^i - t^{i+1})$, and the interior domain of source points are located at the temporal level of $t = t^i - \lambda(t^i - t^{i+1})$, where $i = 1, n-1$ and $\lambda(t^i - t^{i+1})$ is the temporal difference between the source point and field point. Theoretically, the time increment $\Delta t^i = (t^i - t^{i+1})$ could be any positive number, $\Delta t^i > 0$. For convenience, the value of $\Delta t^i, i = 1, n-1$ would be treated as $\Delta t = \Delta t^i, i = 1, n-1$ throughout the process of computation.

By substituting field and source points into (5) and (7), a linear matrix can be formed as

$$A_{ij}\alpha_j = b_i, \text{ for } \quad i, \ j = 1, \ N, \tag{8}$$

where $N = N_f + N_b$ is the number of total computational points, and

$$A_{ij} = \begin{cases} \dfrac{e^{-(\vec{x}_i-\vec{\xi}_j)^2/4\pi\nu(t_i-\tau_j)}}{[4\pi\nu(t_i-\tau_j)]^{d/2}} & \text{if} \quad t_i > \tau_j \\ 0 & \text{if} \quad t_i \le \tau_j \end{cases}. \tag{9}$$

The matrix b_i is a column vector combined with the field values at the given time and boundary conditions. After inverting the matrix, we obtain the under-determined coefficients α, and $U(\vec{x},t)$ is then obtained using (7). The solution at the initial time is then obtained by time evolution.

4 Numerical results

Three different kinds of one-dimensional BHCPs and one two-dimensional BHCP are examined to show the feasibility of time evolution MFS for BHCPs. In addition, in order to test the stability of this method for BHCPs, a random noisy perturbation is added into the given time condition as follows:

$$\sqrt{\frac{1}{N_f}\left(\sum_{i=1}^{N_f}\left(\tilde{g}(\vec{x}_i)-g(\vec{x}_i)\right)^2\right)} \le \left(\frac{s}{100}\right)\max_{\vec{x}\in\{\vec{x}_k\}_{k=1}^{N_f}} \mid g(\vec{x}) \mid, \tag{10}$$

and

$$\sqrt{\frac{1}{N_b}\left(\sum_{i=1}^{N_b}\left(\tilde{f}(t_i)-f(t_i)\right)^2\right)} \le \left(\frac{s}{100}\right)\max_{t\le T} \mid f(t) \mid, \tag{11}$$

where $s\%$ is the percentage of additive noise, $\tilde{g}(\vec{x})$, and $\tilde{f}(t)$ are the prescribed functions with random noise. In the following examples, the time evolution MFS is successfully used to approximate BHCPs without noise, and for noisy problems, the MFS can still be adopted directly as the noise, $s \le 0.1$. But, if the noise, $s > 0.1$, a truncated singular value decomposition (TSVD) technique is combined to treat highly ill-condition BHCPs, where the required parameter is chosen to decrease the effects of noise. Throughout this paper, the maximum absolute error is defined as follows,

$$E = \max_{\vec{x}\in\{\vec{x}_k\}_{k=1}^{N}} \mid U(\vec{x},t) - u(\vec{x},t) \mid,$$

where $U(\vec{x},t)$ and $u(\vec{x},t)$, respectively are the numerical solution and the analytic solution at the k-th interior points.

4.1 Example 1

A one-dimensional benchmark BHCP is listed as

$$\text{PDE:} \quad u_t(x,t) = \nu u_{xx}(x,t), \quad 0 < x < 1, \quad 0 < t < T \tag{12}$$

$$\text{BC:} \quad u(0,t) = u(1,t) = 0, \tag{13}$$

$$\text{FC:} \quad u(x,T) = \sin(\pi x)\exp(-\pi^2 T), \tag{14}$$

where $\nu = 1$, and the analytical solution to this problem is

$$u(x,t) = \sin(\pi x)\exp\left(-\pi^2 t\right), \; 0 \leq t < T. \tag{15}$$

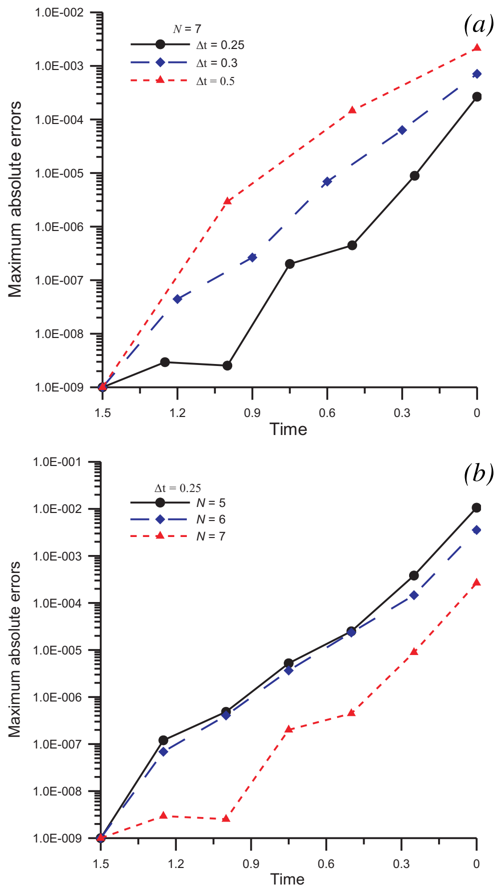

Figure 2: Example 1: (a) Time evolution history of maximum absolute errors for different time increments; and (b) time evolution history of maximum absolute errors for different numbers of points.

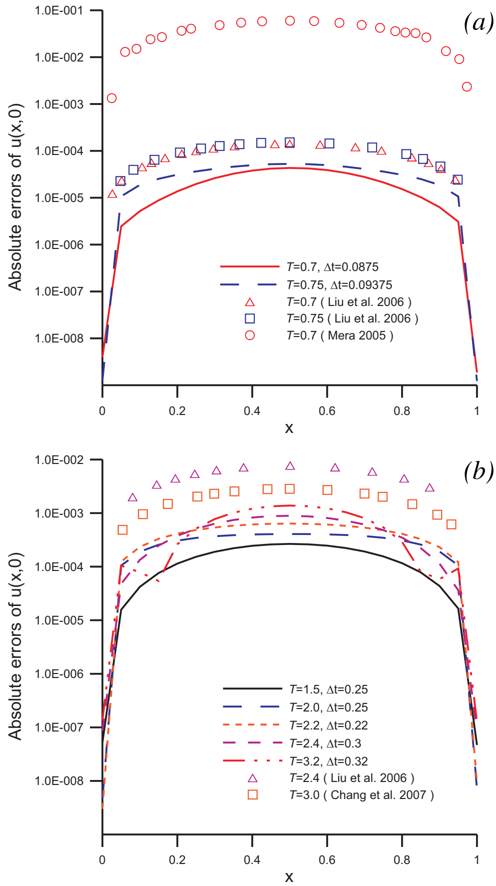

Figure 3: Example 1: (a) The absolute errors at the initial time; and (b) the absolute errors at the initial time.

In order to show the feasibility of the MFS, this BHCP subject to the given time $T = 1.5$ is evaluated with different time increments and computational nodes. Fig. 2a presents the maximum absolute errors with different time increments, Δt, and Fig. 2b presents the maximum absolute errors evaluated at different computational nodes. Increasing the number of computational points or taking smaller time increments yield better results in the numerical computation, as expected. Therefore, we use $N = 7$ computational points to retrieve this BHCP subject to the given time $T = 0.7$ and $T = 0.75$. Fig. 3a shows the absolute errors obtained by the time evolution MFS. Comparing the results with Liu, Chang, and Chang (2006) and Mera (2005), our solutions are obviously more accurate. By using the time evolution scheme, the initial time can be recovered even as the give time T up to $T = 3.2$. The numerical results are shown in Fig. 3b. These results demonstrate that good performance of the method as well as the stability of this approach for a large T.

At the given times from $T = 1.5, 2, 2.2, 2.4$, to 3.2, the field values of this benchmark BHCP are distributed in the range of 10^{-7} to 10^{-13}, when the values at the initial time are in the range of 10^{0}. It is very difficult to recover the initial data when the field values at the given time are so tiny. For such a difficult problem, Lesnic, Elliott, and Ingham (1998) only could obtain solution while $T < 1$. Therefore, we investigate these very severely ill-posed cases to show the significant improvements in the computability of the solutions that are possible using this approach to solve these problems. As shown in Fig. 3b, the results are obtained with $N = 9$, and the solutions demonstrate the improved performance of our method even when solving such a highly ill-posed problem. With $T = 1.5$, the maximum absolute error is as small as 2.661×10^{-4}. Moreover, even at the case with $T = 3.2$, the maximum absolute error still can be kept within 1.383×10^{-3}. Comparing with the same case with Liu, Chang, and Chang (2006) and Chang, Liu, and Chang (2007), our solutions are more accurate and our numerical method is easier to be employed.

In order to test the stability of time evolution MFS, we add some random distributions of noise to the field values at time $T = 1.2$, and use $N = 9$, $\Delta t = 0.24$ to solve it. In Fig. 4a, the matched results obviously show that all of the numerical results in the case with three different levels of noise, including $s = 5$, $s = 10$ and $s = 15$, are close to the exact solution. Meanwhile, the absolute errors in Fig. 4b also present acceptable results, even with a high level noise of 15%. The results demonstrate the excellent performance of the method as well as the stability of this approach for these types of BHCPs.

4.2 Example 2

In this example, another one-dimensional BHCP is considered

$$\text{PDE:} \qquad u_t(x,t) = \nu u_{xx}(x,t), \quad 0 < x < 1, \quad 0 < t < T, \tag{16}$$

$$\text{BC:} \qquad u(0,t) = u(1,t) = 0, \tag{17}$$

$$\text{FC:} \qquad u(x,T) = \sum_{k=0}^{200} \frac{8}{\pi^2 (2k+1)^2} \cos\left(\frac{\pi(2k+1)(2x-1)}{2}\right) \times \xi(T), \tag{18}$$

$$\text{IC:} \qquad u(x,0) = \begin{cases} 2x, & 0 \le x \le 0.5 \\ 2(1-x), & 0.5 \le x \le 1.0 \end{cases}, \tag{19}$$

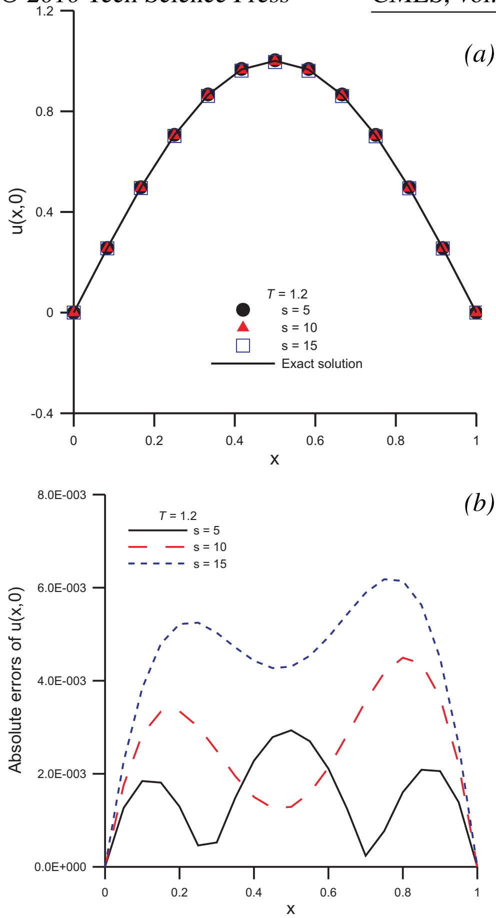

Figure 4: Example 1: (a) The results with different levels of noise compared to the exact solution at the initial time; and (b) the absolute errors with different levels of noise at the initial time.

where $\nu = 1$ and $\xi(T) = \exp\left[-\nu\pi^2(2k+1)^2T\right]$. The analytic solution to the problem posed in (16)–(19) is given by

$$u(x,t) = \sum_{k=0}^{\infty} \frac{8}{\pi^2 (2k+1)^2} \cos\left(\frac{\pi(2k+1)(2x-1)}{2}\right) \times \xi(t), \tag{20}$$

where $\xi(t) = \exp\left[-\nu\pi^2(2k+1)^2t\right]$. The sum in (20) is taken over the first two hundred terms to assure that the analytic solution is obtained within double precision accuracy.

This one-dimensional BHCP is called a triangular test [Muniz, de Campos Velho, and Ramos (1999); Muniz, Ramos, and de Campos Velho (2000); Liu (2004); Liu,

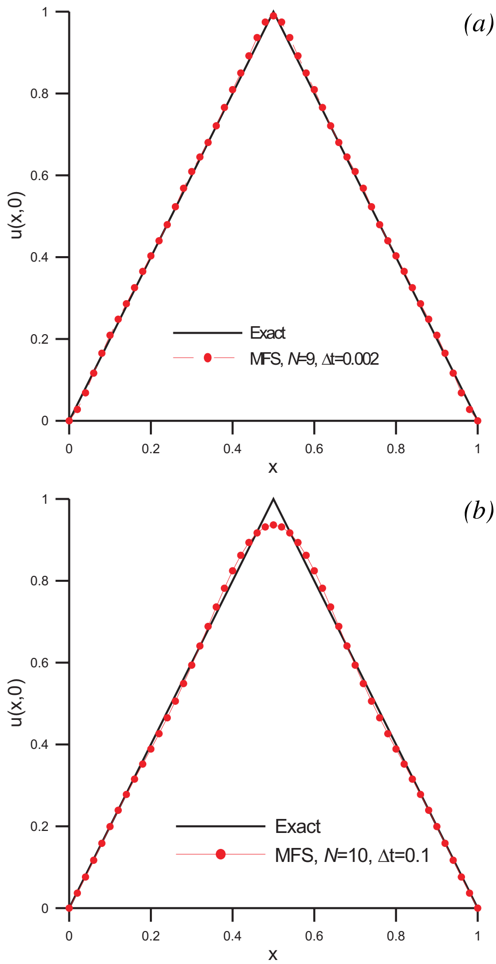

Figure 5: Example 2: (a) The numerical solution compared to the exact solution with $\nu = 1$, $T = 0.01$ at the initial time; and (b) the numerical solution compared to the exact solution with $\nu = 0.1$, $T = 0.5$ at the initial time.

Chang, and Chang (2006); Chiwiacowsky and de Campos Velho (2003)]. In general, it is very difficult for other numerical computational methods to use smooth field values at the given time $t = T$ in (18) to recover non-smooth values at the initial time in (19). In this numerical example, we solve the triangular test problem with $\nu = 1$, $T = 0.01$, $N = 9$ and the time increment, $\Delta t = 0.002$. Despite these difficulties, accurate results were obtained, and these are presented in Fig. 5a. Without combining the basic approach with any regularization method, the maximum absolute error was 9.35×10^{-3}, and this occurred at $x = 0.5$, i.e., at the apex of the triangle, as would be expected. For an even more ill-conditioned problem

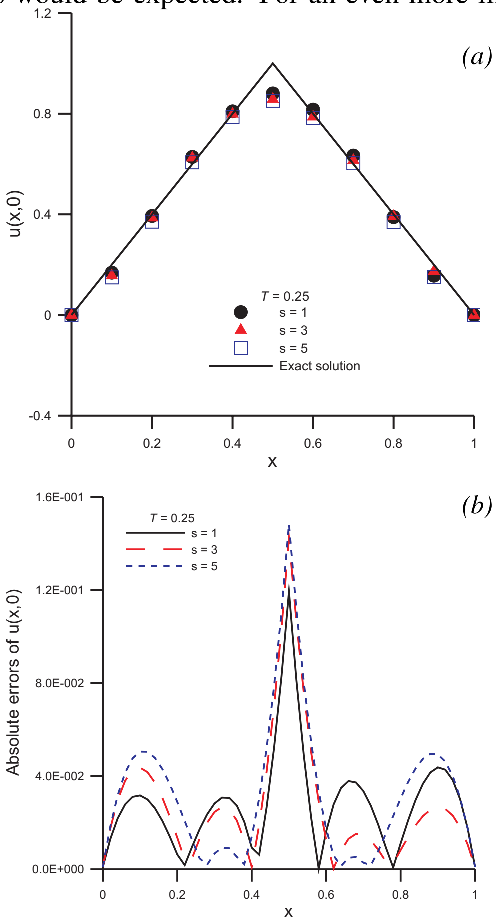

Figure 6: Example 2: (a) The results with different levels of noise compared to the exact solution at the initial time; and (b) the absolute errors with different levels of noise at the initial time.

with $\nu = 0.1$ and $T = 0.5$, Muniz, de Campos Velho, and Ramos (1999); Muniz, Ramos, and de Campos Velho (2000) cannot obtain satisfactory results at the given time, $T = 0.008$. In Fig. 5b, using $N = 10$ and $\Delta t = 0.1$ yields our scheme usable results even at the turning point, $x = 0.5$, where the maximum absolute error is 1.72×10^{-2}.

As a final challenge in this difficult case, we also added some random perturbations with $s = 1$, $s = 3$ and $s = 5$ to the solution at time $T = 0.25$ to test the stability of the time evolution MFS. In Fig. 6a, $N = 10$ and $\Delta t = 0.05$ are used, and each of the numerical results approximates the corresponding exact solution within an acceptable range except at the non-smooth point. At the same time, the absolute error in Fig. 6b shows the results are of sufficiently high quality to assert the superiority of the approach as a means to solve these types of problems.

4.3 Example 3

An one-dimensional BHCP is considered as

$$\text{PDE:} \quad u_t(x,t) = \nu u_{xx}(x,t), \quad -\pi < x < \pi, \quad 0 < t < T, \tag{21}$$

$$\text{BC:} \quad u(-\pi,t) = u(\pi,t) = 0, \tag{22}$$

$$\text{FC:} \quad u(x,T) = e^{-\beta^2 T} \sin \beta x, \tag{23}$$

where $\nu = 1$, $\beta \in \mathbb{N}$ and the exact solution is obtained from

$$u(x,t) = e^{-\beta^2 t} \sin \beta x. \tag{24}$$

Liu, Chang, and Chang (2006) demonstrated that the solution of this ill-posed problem does not depend on the final data continuously, and also mentioned that this kind of BHCP is unstable for a given final data with large β. In another words, the problem becomes more ill-posed when β is large. In this case, when $\beta = 3$ and $T = 1$, the desired initial field value is $\sin 3x$ and value at the given time is $e^{-9} \sin 3x$. The value of $\sin 3x$ is on the order of 10^0, and the value of $e^{-9} \sin 3x$ is on the order of 10^{-4}. For this example, it is very difficult to retrieve the initial value from the rather small field value as 10^{-4}. Liu, Chang, and Chang (2006) also remarked that it is impossible to solve this strongly ill-posed problem with classical numerical methods. In Fig. 7a, we obtain results with $N = 12$ and $\Delta t = 0.25$ to compare with the exact solution from (24) at the initial time. The absolute errors are on the order of 10^{-3}, and as shown in Fig. 7b, the maximum absolute error is less than 5×10^{-3}. In this problem, $N = 12$ computational points and $\Delta t = 0.05$ are used, and random noise is added at $T = 0.25$ with $s = 5$, $s = 8$ and $s = 10$ to show the time evolution MFS is stable enough to overcome these different levels of noise. In Fig. 8a, the results obtained with different levels of noise closely match the solid line of the exact solution. In Fig. 8b, the absolute errors show acceptable results even with high levels of noise. These results demonstrate that time evolution is accurate and stable enough to solve these types of BHCPs.

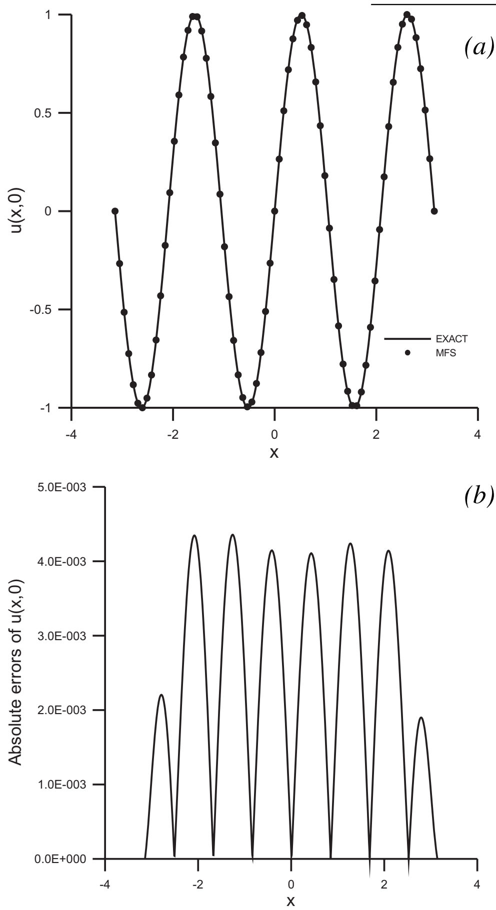

Figure 7: Example 3: (a) The numerical solution compared to the exact solution with $T = 1$; and (b) the absolute errors with $T = 1$ at the initial time.

4.4 Example 4

We further consider a two-dimensional BHCP,

$$\text{PDE:} \quad u_t(x,y,t) = \nu \nabla^2 u(x,y,t), \ -\pi < x < \pi, \ -\pi < y < \pi, \ 0 < t < T, \tag{25}$$

$$\text{BC:} \quad u(-\pi,y,t) = u(\pi,y,t) = u(x,-\pi,t) = u(x,\pi,t) = 0, \tag{26}$$

$$\text{FC:} \quad u(x,y,T) = e^{-2\beta^2 T} \sin\beta x \sin\beta y, \tag{27}$$

where $\nu = 1$, $\beta \in \mathrm{N}$ is a positive integer, and the exact solution is

$$u(x,y,t) = e^{-\beta^2 t} \sin\beta x \sin\beta y. \tag{28}$$

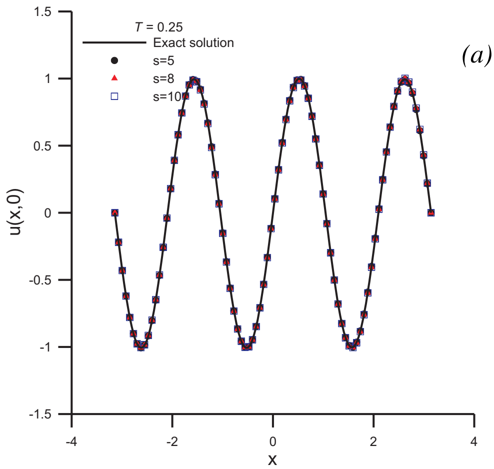

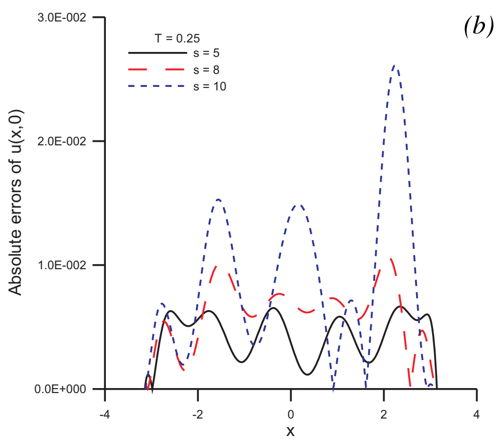

Figure 8: Example 3: (a) The results with different levels of noise compared to the exact solution at the initial time; and (b) the absolute errors with different levels of noise at the initial time.

In this case, $N = 64$ and $\Delta t = 0.2$ are used to solve this problem with, $\beta = 1$ and $T = 1$. In Fig. 9, all of the absolute errors between the exact solution and the numerical results are within 5×10^{-5}. Moreover, we draw the absolute errors at $x = -\pi + 134\pi/90$ and $y = -\pi + 148\pi/90$ to clearly show the accuracy in detail. In Fig. 10a, each absolute error can reach the accuracy on the order of 10^{-5}. Comparing the distribution of absolute errors to those cited in Liu, Chang, and Chang (2006), our solution is more accurate.

In this two-dimensional problem, we also add additional random noise to the solution at $T = 0.25$, and $N = 64$, $\Delta t = 0.05$ are adopted. In Fig. 10b, we can recover the solution at the initial time with $s = 8$ and $s = 10$ of noise levels. Obtaining accepted results with such high level of noise in BHCP has been impossible without using this scheme.

5 Conclusions

The time evolution MFS is successfully used to solve backward heat conduction problems with diffusion fundamental solutions. Using time evolution provides significant numerical advantages. Not only does it help to decrease the computing errors due to ill-conditioning, but also makes it possible to directly obtain numerical solutions of the BHCPs without regularization. The use of time-stepping formulations has an extensive history in the numerical solution of PDEs, and the approach has proven to be productive in solving even steady state problems with weak solutions. The excellent numerical results obtained in this study demonstrate the accuracy and feasibility of extending this numerical technique to solve the BHCPs.

Demonstrating the ability to solve idealized problems with exact analytical solutions is interesting. For engineering utility, however the addition of noise to these types of problems is of even greater importance, as it can be expected that the nu-

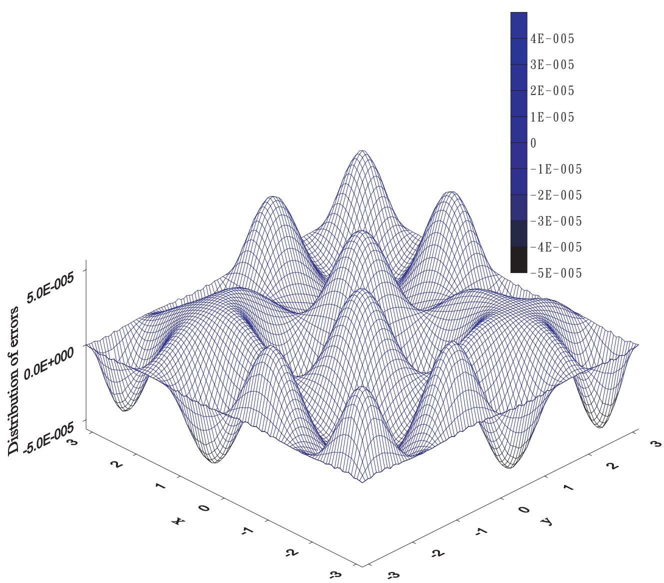

Figure 9: Example 4: The errors between the exact solution and the numerical results are plotted showing the distribution of the errors on the domain. Note that all of the errors are within 5×10^{-5}.

merical data used to solve backward heat conduction problems will almost certainly contain noise. The approach which we outlined in this paper seems to provide a workable solution to a range of problems containing additive noise that we have investigated. We also successfully combined the TSVD technique to avoid the amplified error due to the ill-conditioning of the BHCPs.

The stability of the time evolution MFS is demonstrated, as the method successfully recovered solutions at the initial time for BHCPs with at least $s = 5$ of noise. Moreover, the method can be used even for some problems with very high levels of noise, e.g., $s = 15$. In summary we have shown conclusively that time evolution

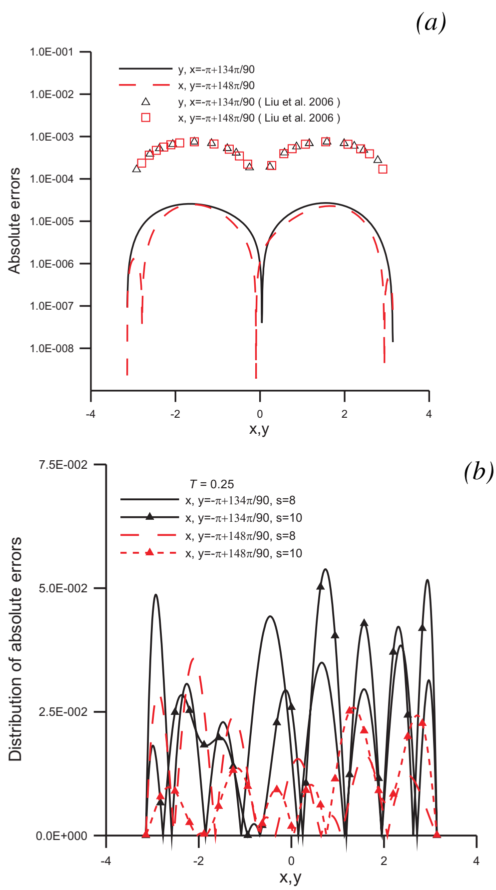

Figure 10: Example 4: (a) The absolute errors are plotted with $T = 1$ and $\beta = 1$; and (b) the absolute errors with $s = 8$, $s = 10$ of noise at the initial time. The solid lines represents the errors respect to y at $x = -\pi + 134\pi/90$, and the dashed lines represents the errors respect to x at $y = -\pi + 148\pi/90$.

MFS is a stable, powerful and suitable numerical method for solving a wide variety of BHCPs. To extend the present algorithm to multi-dimensional BHCPs, such as 3D problems is a straightforward task without extra effort and is undertaking. The results will be reported in the future.

Acknowledgement: This research was partially supported by the National Science Council in Taiwan through Grant NSC 96-2622-E-002-017-CC3 and NSC 96-2221-E-002-116-.

References

Chang, C. W.; Liu, C. S. (2010): A backward group preserving scheme for multi-dimensional backward heat conduction problems . *CMES: Computer Modeling in Engineering & Sciences*, vol. 59, pp. 239–274.

Chang, J. R.; Liu, C. S.; Chang, C. W. (2007): A new shooting method for quasi-boundary regularization of backward heat conduction problems. *Int. J. Heat Mass Transf.*, vol. 50, no. 11-12, pp. 2325–2332.

Chiwiacowsky, L. D.; de Campos Velho, H. F. (2003): Different approaches for the solution of a backward heat conduction problem. *Inverse Probl. Eng*, vol. 11, no. 6, pp. 471–494.

Fenner, R. T. (1991): Source field superposition analysis of two-dimensional potential problems. *Int. J. Numer. Methods Eng.*, vol. 32(5), pp. 1079–1091.

Han, H.; Ingham, D. B.; Yuan, Y. (1995): The boundary-element method for the solution of the backward heat-conduction equation. *J. Comput. Phys.*, vol. 116, no. 2, pp. 292–299.

Hon, Y. C.; Li, M. (2009): A discrepancy principle for the source points location in using the MFS for solving the BHCP. *Int. J. Comput. Methods*, vol. 6, no. 2, pp. 181–197.

Hon, Y. C.; Wei, T. (2005): The method of fundamental solution for solving multidimensional inverse heat conduction problems. *CMES: Computer Modeling in Engineering & Sciences*, vol. 7, no. 2, pp. 119–132.

Hu, S. P.; Young, D. L.; Fan, C. M. (2008): FDMFS for diffusion equation with unsteady forcing function . *CMES: Computer Modeling in Engineering & Sciences*, vol. 24, pp. 1–20.

Karageorghis, A.; Fairweather, G. (2000): The method of fundamental solutions for axisymmetric elasticity problems. *Comput. Mech.*, vol. 25(6), pp. 524–532.

Kita, E.; Kamiya, N. (1995): Trefftz method: an overview. *Adv. Eng. Softw.*, vol. 24, pp. 3–12.

Koopmann, G. H.; Song, L. M.; Fahnline, J. B. (1989): A method for computing acoustic fields based on the principle of wave superposition. *J. Acoust. Soc. Am.*, vol. 86, no. 6, pp. 2433–2438.

Kupradze, V. D.; Aleksidze, M. A. (1964): The method of functional equations for the approximate solution of certain boundary value problems. *USSR Comput. Math. Math. Phys*, vol. 4, pp. 82–126.

Kythe, P. K. (1996): *Fundamental solutions for differential operators and applications*. Birkhauser, Boston.

Lesnic, D.; Elliott, L.; Ingham, D. B. (1998): An iterative boundary element method for solving the backward heat conduction problem using an elliptic approximation. *Inverse Probl. Sci. Eng.*, vol. 6(4), pp. 255–279.

Liu, C. S. (2004): Group preserving scheme for backward heat conduction problems. *Int. J. Heat Mass Transf.*, vol. 47, no. 12-13, pp. 2567–2576.

Liu, C. S. (2008): Improving the ill-conditioning of the method of fundamental solutions for 2D Laplace equation. *CMES: Computer Modeling in Engineering & Sciences*, vol. 28, pp. 77–93.

Liu, C. S.; Chang, C. W.; Chang, J. R. (2006): Past cone dynamics and backward group preserving schemes for backward heat conduction problems. *CMES: Computer Modeling in Engineering & Sciences*, vol. 12, no. 1, pp. 67–81.

Marin, L. (2008): Stable MFS solution to singular direct and inverse problems associated with the Laplace equation subjected to noisy data. *CMES: Computer Modeling in Engineering & Sciences*, vol. 37, no. 2, pp. 203–242.

Marin, L. (2008): The method of fundamental solutions for inverse problems associated with the steady-state heat conduction in the presence of sources. *CMES: Computer Modeling in Engineering & Sciences*, vol. 30, no. 2, pp. 99–122.

Mera, N. S. (2005): The method of fundamental solutions for the backward heat conduction problem. *Inverse Probl. Sci. Eng.*, vol. 13, no. 1, pp. 65–78.

Mera, N. S.; Elliott, L.; Ingham, D. B.; Lesnic, D. (2000): An iterative boundary element method for the solution of a Cauchy steady state heat conduction problem. *CMES: Computer Modeling in Engineering & Sciences*, vol. 1, no. 3, pp. 101–106.

Muniz, W. B.; de Campos Velho, H. F.; Ramos, F. M. (1999): A comparison of some inverse methods for estimating the initial condition of the heat equation. *J. Comput. Appl. Math.* , vol. 103, no. 1, pp. 145–163.

Muniz, W. B.; Ramos, F. M.; de Campos Velho, H. F. (2000): Entropy- and tikhonov-based regularization techniques applied to the backwards heat equation. *Comput. Math. Appl.*, vol. 40, pp. 1071–1084.

Smyrlis, Y. S.; Karageorghis, A. (2003): Some aspects of the method of fundamental solutions for certain biharmonic problems. *CMES: Computer Modeling in Engineering & Sciences*, vol. 4, no. 5, pp. 535–550.

Trefftz, E. (1926): Ein gegenstuck zum ritzschen verfahren. in proceedings of the 2nd international congress of applied mechanics, zurich, 1926. orell fussli verlag. In *131-137*.

Young, D. L.; Ruan, J. W. (2005): Method of fundamental solutions for scattering problems of electromagnetic waves. *CMES: Computer Modeling in Engineering & Sciences*, vol. 7, pp. 223–232.

Young, D. L.; Tsai, C. C.; Fan, C. M. (2004): Direct approach to solve non-homogeneous diffusion problems using fundamental solutions and dual reciprocity methods. *J. Chin. Inst. Eng.*, vol. 27(4), pp. 597–609.

Young, D. L.; Tsai, C. C.; Murugesan, K.; Fan, C. M.; Chen, C. W. (2004): Time-dependent fundamental solutions for homogeneous diffusion problems. *Eng. Anal. Bound. Elem.*, vol. 28, no. 12, pp. 1463–1473.